STATE UNIVERSITY OF NEW YORK
AT STONY BROOK

Image Deblurring and Aperture Synthesis Using a Posteriori Processing by Fourier-Transform Holography, G. W. Stroke

Technical Report No. 189

College of Engineering

OPTICA ACTA, 1969, VOL. 16, NO. 4, 401–422

Image deblurring and aperture synthesis using *a posteriori* processing by Fourier-transform holography†

GEORGE W. STROKE
Electro-Optical Sciences Center, State University of New York, Stony Brook, New York 11790, U.S.A.

(*Received* 22 *November* 1968)

Abstract. Two forms of holographic spatial filtering may be used for the deconvolution of accidentally blurred images and of images deliberately 'coded' for aperture-synthesis purposes. The first is generally applicable and uses a Fourier-transform division filter realized by holography from the instrumental 'spread function' of the system. The second, even more straightforward, is particularly suited for the special case when the autocorrelation function of the spread function is or may suitably be made to be sharply peaked. This form should permit one to realize a new class of optical systems in cases where conventional (lens and mirror) systems may not be readily realized (e.g. for X-ray and ultrasonic imaging, for space astronomy and photography, among others). Previously unpublished, new theoretical and experimental results are given. Applications to the possibilities of achieving 'super-resolutions' and for solving the 'phase problem' in X-ray crystallography are also briefly mentioned.

1. Introduction

Recent work has demonstrated that it is possible to extract greatly sharpened 'deblurred' images from photographs which have been blurred by accident or deliberately coded, for instance in view of 'aperture synthesis' applications [1–8]. The blurring or coding of the blurred photograph $g(x, y)$ may be expressed as the spatial convolution:

$$g(x', y') = \int\int_{-\infty}^{+\infty} f(x, y)\, h(x' - x, y' - y)\, dx\, dy, \tag{1}$$

between the desired image $f(x, y)$ and the instrumental impulse response function (spread function, i.e. image of a point) $h(x, y)$. It is well known that equation (1) takes on the form of the product:

$$\bar{G}(u, v) = \bar{F}(u, v)\, \bar{H}(u, v), \tag{2}$$

in the spatial Fourier-transform domain‡, where we have:

$$\bar{F}(u, v) = \int\int_{-\infty}^{+\infty} f(x, y) \exp\left[2\pi i(ux + vy)\right] dx\, dy \tag{3}$$

and similarly for $\bar{G}$ and $\bar{H}$, with suitable normalization‡. It is also well known that a Fourier-transform relation such as that of equation (3) exists between the

† Presented on 24 September 1968, by invitation, at the International Commission for Optics Symposium on Applications of Coherent Light, in Florence, Italy.

‡ For a general background, notations and approximations used see, e.g.

STROKE, G. W., 1966, *An Introduction to Coherent Optics and Holography* (New York: Academic Press); second, revised and enlarged edition, December 1968.

STROKE, G. W., 1967, *Handbuch der Physik*, Vol. 29, edited by S. Flügge (Berlin: Springer Verlag), pp. 426–754, notably pp. 504–570.

and the transmission of this positive (P) is:

$$\bar{E}_T = [g(x,y)^{-\gamma_N}]^{-\gamma_P/2} = g(x,y), \quad [\gamma_N \gamma_P = 2] \tag{13}$$

if the condition of equation (11) is satisfied.

Finally, as we recall below, with particular reference to this work, it is now well known (see, e.g. [8]), that the three angularly separated waves, produced by holograms, have electric field-vector amplitudes which can readily be made to be *independent* of the photographic recording and processing conditions under some specified conditions. For instance, let $\bar{E}_O(u,v)$ describe the field produced by the 'object' field in the plane (u,v) of the hologram, and let $\bar{E}_R(u,v)$ be the field similarly produced by the 'reference' source in the hologram plane. The exposure of the hologram is (with the time-averaging understood):

$$I(u,v) = (\bar{E}_O + \bar{E}_R)(\bar{E}_O + \bar{E}_R)^*, \tag{14}$$

i.e. in the well-known form:

$$I(u,v) = [|\bar{E}_O|^2 + |\bar{E}_R|^2] + [\bar{E}_O \bar{E}_R^*] + [\bar{E}_O^* \bar{E}_R], \tag{15}$$

where the three separated waves have been separately bracketed. The electric field vector distribution of the field transmitted through the hologram, processed with a γ, may be made to be *proportional* to $I(u,v)$, with the γ appearing only as a scale factor, provided only that one respects the simple condition:

$$|\bar{E}_R|^2 \gg |\bar{E}_O|^2. \tag{16}$$

In practice, the condition $\gg$ may mean approximately:

$$|\bar{E}_R|^2 \cong (4 \text{ to } 10)|\bar{E}_O|^2,$$

as an example. Indeed, if we write equation (15) in the form:

$$I(u,v) = |\bar{E}_R|^2 \left\{ 1 + \frac{|\bar{E}_O|^2}{|\bar{E}_R|^2} + \frac{\bar{E}_O}{\bar{E}_R} + \frac{\bar{E}_O^*}{\bar{E}_R^*} \right\} \tag{17}$$

and if we recall that the electric field transmitted through the hologram (negative!) is (upon illumination with a wave of unit amplitude):

$$\bar{E}_T = I(u,v)^{-\gamma_N/2}, \tag{18}$$

we readily see, by a binomial expansion of equation (18), that the form $(1+\epsilon)$, with ϵ small, of equation (17) gives:

$$\bar{E}_T \cong |\bar{E}_R|^{-\gamma_N} \left\{ 1 - \frac{\gamma_N}{2} \left[\frac{|\bar{E}_O|^2}{|\bar{E}_R|^2} + \frac{\bar{E}_O}{\bar{E}_R} + \frac{\bar{E}_O^*}{\bar{E}_R^*} \right] \right\}, \tag{19}$$

i.e.

$$\bar{E}_T \cong |\bar{E}_R|^{-\gamma_N - 2} \left[|\bar{E}_R|^2 - \frac{\gamma_N}{2} |\bar{E}_O|^2 \right]$$

$$- \frac{\gamma_N}{2} |\bar{E}_R|^{-\gamma_N - 2} [\bar{E}_O \bar{E}_R^*]$$

$$- \frac{\gamma_N}{2} |\bar{E}_R|^{-\gamma_N - 2} [\bar{E}_O^* \bar{E}_R]. \tag{20}$$

spatial part of the complex electric field amplitude $\bar{E}(x, y)$ in the pupil of a perfectly corrected (ideal) lens system and the field $\bar{E}(u, v)$ in the image plane (u, v)†, i.e.

$$\bar{E}(u, v) = \int\int_{-\infty}^{+\infty} \bar{E}(x, y) \exp\left[2\pi i(ux + vy)\right] dx\, dy. \tag{4}$$

It is also known that one may readily realize by transmission through a photographic transparency an electric field vector distribution $\bar{E}_T(x, y)$ equal to the exposure $g(x, y)$ of a photographic transparency, i.e.

$$\bar{E}_T(x, y) = g(x, y) \tag{5}$$

by suitable processing of the photographic negative exposed to the 'intensity' $g(x, y)$, where we have

$$g(x, y) = \langle \tilde{\bar{E}}(x, y, t)\, \tilde{\bar{E}}^*(x, y, t) \rangle \tag{6}$$

under the usual assumptions [see Stroke, *loc. cit.* 1966, 1967, 1968), and similarly for the spread function $h(x, y)$. For instance, in the linear range of the Hurter and Driffield curve, where the slope is $\tan^{-1}\gamma_N$, and where we have

$$\log \frac{1}{|\bar{E}_T|^2} = \gamma_N \log g(x, y) \tag{7}$$

the 'amplitude' transmission of the negative exposed to $g(x, y)$ is

$$|\bar{E}_T| = g(x, y)^{-\gamma_N/2}, \tag{8}$$

By taking suitable care, it is possible to make the phase transmission of the negative to be a constant, so that we may write:

$$\bar{E}_T(x, y) = g(x, y)^{-\gamma_N/2}. \tag{9}$$

It should be clear (as first pointed out by Gabor [14]) that we may make

$$\bar{E}_T(x, y) = g(x, y) \quad [\gamma_N = -2] \tag{10}$$

with the condition $\gamma_N = -2$‡. In practice [1] this condition may be realized by making a contact print of the negative (N), and by processing this positive (P) in such a way that the condition:

$$\gamma_N \gamma_P = 2, \tag{11}$$

be satisfied. In other words, the exposure of the positive P is:

$$[g(x, y)^{-\gamma_N/2}]^2 = g(x, y)^{-\gamma_N} \tag{12}$$

† For a general background, notations and approximations used see, e.g., G. W. Stroke (1966, 1967), *op. cit.*

‡ Another way of expressing the relation between the transmittance of the photographic plate and the exposure (kindly suggested by one referee) is as follows: One may readily realize an amplitude transmission $t(x, y)$ of a photographic emulsion proportional to the exposure $E(x, y)$ by suitable processing. The exposure is proportional to the intensity:

$$I = \langle \mathbf{E}(x, y, t) \cdot \mathbf{E}^*(x, y, t) \rangle.$$

In the linear range of the Hurter and Driffield curve, where the slope is $\tan^{-1}\gamma$ and where we have the equation $\log(1/T) = \gamma \log E(x, y)$ the intensity transmission is

$$T(x, y) = \text{const. } I^{-\gamma}$$

and the amplitude transmission:

$$t(x, y) = [T(x, y)]^{1/2} = \text{const. } I^{-1/2\gamma}$$

and by making $\gamma = -2$ the amplitude transmission $t(x, y)$ becomes proportional to E.

and the transmission of this positive (P) is:

$$\bar{E}_T = [g(x,y)^{-\gamma_N}]^{-\gamma_P/2} = g(x,y), \quad [\gamma_N \gamma_P = 2] \tag{13}$$

if the condition of equation (11) is satisfied.

Finally, as we recall below, with particular reference to this work, it is now well known (see, e.g. [8]), that the three angularly separated waves, produced by holograms, have electric field-vector amplitudes which can readily be made to be *independent* of the photographic recording and processing conditions under some specified conditions. For instance, let $\bar{E}_O(u,v)$ describe the field produced by the 'object' field in the plane (u,v) of the hologram, and let $\bar{E}_R(u,v)$ be the field similarly produced by the 'reference' source in the hologram plane. The exposure of the hologram is (with the time-averaging understood):

$$I(u,v) = (\bar{E}_O + \bar{E}_R)(\bar{E}_O + \bar{E}_R)^*, \tag{14}$$

i.e. in the well-known form:

$$I(u,v) = [|\bar{E}_O|^2 + |\bar{E}_R|^2] + [\bar{E}_O \bar{E}_R^*] + [\bar{E}_O^* \bar{E}_R], \tag{15}$$

where the three separated waves have been separately bracketed. The electric field vector distribution of the field transmitted through the hologram, processed with a γ, may be made to be *proportional* to $I(u,v)$, with the γ appearing only as a scale factor, provided only that one respects the simple condition:

$$|\bar{E}_R|^2 \gg |\bar{E}_O|^2. \tag{16}$$

In practice, the condition $\gg$ may mean approximately:

$$|\bar{E}_R|^2 \cong (4 \text{ to } 10)|\bar{E}_O|^2,$$

as an example. Indeed, if we write equation (15) in the form:

$$I(u,v) = |\bar{E}_R|^2 \left\{1 + \frac{|\bar{E}_O|^2}{|\bar{E}_R|^2} + \frac{\bar{E}_O}{\bar{E}_R} + \frac{\bar{E}_O^*}{\bar{E}_R^*}\right\} \tag{17}$$

and if we recall that the electric field transmitted through the hologram (negative!) is (upon illumination with a wave of unit amplitude):

$$\bar{E}_T = I(u,v)^{-\gamma_N/2}, \tag{18}$$

we readily see, by a binomial expansion of equation (18), that the form $(1+\epsilon)$, with ϵ small, of equation (17) gives:

$$\bar{E}_T \cong |\bar{E}_R|^{-\gamma_N} \left\{1 - \frac{\gamma_N}{2}\left[\frac{|\bar{E}_O|^2}{|\bar{E}_R|^2} + \frac{\bar{E}_O}{\bar{E}_R} + \frac{\bar{E}_O^*}{\bar{E}_R^*}\right]\right\}, \tag{19}$$

i.e.

$$\bar{E}_T \cong |\bar{E}_R|^{-\gamma_N - 2}\left[|\bar{E}_R|^2 - \frac{\gamma_N}{2}|\bar{E}_O|^2\right] - \frac{\gamma_N}{2}|\bar{E}_R|^{-\gamma_N - 2}[\bar{E}_O \bar{E}_R^*] - \frac{\gamma_N}{2}|\bar{E}_R|^{-\gamma_N - 2}[\bar{E}_O^* \bar{E}_R]. \tag{20}$$

This equation must be carefully considered for the purposes of this paper. First, we may note that the field $\bar{E}_T$ transmitted through the hologram (upon illumination with a wave of unit amplitude) will indeed have its imaging waves proportional to $[\bar{E}_O \bar{E}_R^*]$ and $[\bar{E}_O^* \bar{E}_R]$, i.e.

$$-\frac{\gamma_N}{2} |\bar{E}_R|^{-\gamma_N - 2} [\bar{E}_O \bar{E}_R^*] \propto \bar{E}_O \bar{E}_R^* \tag{21}$$

and

$$-\frac{\gamma_N}{2} |\bar{E}_R|^{-\gamma_N - 2} [\bar{E}_O^* \bar{E}_R] \propto \bar{E}_O^* \bar{E}_R, \tag{22}$$

to the extent that the amplitude $|\bar{E}_R(u, v)|$ of the reference wave may be considered as constant in the hologram plane. The condition [$|\bar{E}_R| = \text{const.}$] may, in practice be readily realized for a number of unfocused waves. This will be the case for a plane wave (originating from a point source 'at infinity'), a spherical wave (e.g. as originating from a point source near the object). In fact, as may be readily verified by experiment, most fields in which the object is not focused on the plate encountered in optics (as distinguished from a field near a source, in a 'focused' image region, in shadows, etc.) happens to have an amplitude which is uniform, i.e. constant, over very extended regions! In particular, the far-field region of an 'extended' reference source, as we use it in holography, as well as the field produced by it by Fourier transformation, both have amplitudes which may be considered as constant, within the requirements of equations (21) and (22). Under these conditions, we may henceforth write that the field transmitted by the hologram of equation (15) upon illumination with a wave $\bar{E}_{R'}(u, v)$ is:

$$\bar{E}_T(u, v) \propto \bar{E}_{R'}(u, v) I(u, v), \tag{23}$$

i.e.

$$\begin{aligned} \bar{E}_T(u, v) \propto \bar{E}_{R'} [|\bar{E}_O|^2 + |\bar{E}_R|^2] \\ + \bar{E}_O \bar{E}_R^* \bar{E}_{R'} \\ + \bar{E}_O^* \bar{E}_R \bar{E}_{R'}. \end{aligned} \tag{24}$$

Because of the Fourier-transforming property of lenses, as expressed in equation (4) and because of the possibilities of obtaining linear relations between the fields transmitted by a photographic transparency and its exposure (equation (13)) on the one hand, and on the other, between the field transmitted by a hologram and its exposure (equation (24)), we shall show that Fourier-transform holography [9], and notably 'extended-source Fourier-transform holography' [11, 12] offer a particularly straight-forward solution to the 'inversion' of the integral equation (1).

Indeed, if we write the integral equation (1) in the symbolic form†:

$$g(x, y) = f(x, y) \otimes h(x, y), \tag{25}$$

where $\otimes$ indicates a spatial convolution [8], and if we recall the Fourier-transform equivalent of equation (25):

$$\bar{G}(u, v) = \bar{F}(u, v) \bar{H}(u, v), \tag{2}$$

† The notation used is that introduced by:
BRACEWELL, R. N., 1965, *The Fourier Transform and its Applications* (New York: McGraw-Hill Book Company). See also [8].

then it should be clear that the desired image $f(x,y)$ may be extracted from the photograph $g(x,y)$, provided that we can 'extract' the function $\bar{F}(u,v)$ from the function $\bar{G}(u,v)$, and take the Fourier transform of $\bar{F}(u,v)$, for instance with another lens. That this should be possible, in principle, was first suggested by Maréchal and Croce [12] in 1953, and again, at that time for the purposes of improving on the spectra produced by insufficiently perfect diffraction gratings, by the author [7] in 1955, who also proposed a solution in the form of a Fourier-transform 'division' as we discuss below. However, it was only when we realized [1] that *holograms*, as first described by Gabor [13–15] in 1948, could be readily used to help in the *realization* (materialization) of the required spatially-complex filters, that the practical solutions, such as those which we present with new theoretical and experimental detail below, became possible†.

In brief, two methods permit one to extract the function $\bar{F}(u,v)$ from the function $\bar{G}(u,v)$ of equation (2), and from it, by a second Fourier transformation, the desired image function $f(x,y)$.

One method [1] consists in *dividing* $\bar{G}(u,v)$ by the function $\bar{H}(u,v)$, i.e. by performing the operation:

$$\bar{G}\bar{H}^{-1}=\bar{F} \tag{26}$$

This method, as may be readily shown, is quite general, and permits one to retrieve the desired function to the limit of 'diffraction' of the original focusing system, already in the first step. The method does require, however, considerable care in the photographic steps involved, as we show below.

Another method, recently originated by the author [5, 6] appears to be much more powerful, as well as considerably simpler. Its application to the special case of image 'deblurring', for images formed by initially 'well-corrected' systems, which were out-of-focus or moved during the exposure, is less general than the Fourier-transform division method, but much simpler to implement, at the present stage of development. Moreover, we show below that the second method has already formed the basis for the design of a new class of optical systems which, by themselves are, paradoxically, rather poor (deliberately poor) image-forming systems, as far as the formation of the first-step photograph $g(x,y)$ is concerned. This second method of image deconvolution (decoding) consists, in one form, of *multiplying* the function $\bar{G}(u,v)$ by the complex conjugate $\bar{H}^*(u,v)$ of the function $\bar{H}(u,v)$, where we recall that $\bar{H}(u,v)$ is the spatial Fourier transform of the spread function $h(x,y)$, according to equation (3). The second method of image deconvolution is described by the equation [5, 6]:

$$\bar{G}\bar{H}^*=\bar{F}\bar{H}\bar{H}^*=\bar{F}, \tag{27a}$$

if

$$\bar{H}\bar{H}^*=1. \tag{27b}$$

According to a well-known theorem (see, e.g. [8]), the 'decoding' condition:

$$\bar{H}\bar{H}^*=1, \tag{27b}$$

may be written in the (x,y) domain in the form:

$$\int\int_{-\infty}^{+\infty} h(x,y)\,h^*(x+x',y+y')\,dx\,dy=\delta(x',y'), \tag{28}$$

† In this work, the Fourier-transform holograms have been recorded with rather than without the use of a lens [9 *a*].

where (x', y') is the Dirac delta function. We may write equation (28) in the equivalent symbolic form (see [8]):

$$h \asymp h^* = \delta \tag{29}$$

where the symbol $\asymp$ indicates (here) the spatial autocorrelation operation described by equation (28). The conditions (27 *b*) and (29) which must be satisfied in order that the operation $\bar{G}\bar{H}^*$ may indeed yield $\bar{F}$ as desired, according to equation (27 *a*), may be formally related by the Fourier-transform theorem:

$$\bar{H}\bar{H}^* \rightleftharpoons h \asymp h^*, \tag{30}$$

referred to above, where the symbol $\rightleftharpoons$ indicates 'by Fourier transformation'. It may be helpful to recall that the 'decoding' conditions $\bar{H}\bar{H}^* = 1$ (equation (27 *a*)), i.e. $h \asymp h^* = \delta$ (equation (29)) are in fact extensions of the method of 'extended-source Fourier-transform holography', (see [10, 11] and [8, pp. 127–137]). A particularly remarkable example of a function described by equation (29), suggested by Gabor [40], is that of a simple diffusing (ground) glass. This is further illustrated in figure 3.

In the sections which follow, we continue to present, as above, only such new aspects of our work which we have not extensively presented elsewhere. Further details with regard to the second method, which we may call the 'correlative holographic decoding method', appear in [5, 6, 16]. Similarly, we may call the first method the 'holographic Fourier-transform division method', for short. Before proceeding to the discussion of these methods, with their experimental illustrations, it may be in order to make some reference to the advantages in speed which these optical computing methods have in comparison with digital-computer solutions of the deconvolution problem, e.g. as demonstrated by Harris [17] since 1966. According to Ansley [18], the Fourier-transform deconvolution of an aerial photograph, 4×4 in. square, with a resolution of 150 lines/mm (i.e. $2{\cdot}25 \times 10^8$ bits) would require 15 hours of computing time, on the fastest presently available computer, IBM 360 Model 67 (having a 6 μsec multiply + add time), even with the use of the powerful Cooley–Tukey algorithm [19], which reduces the computational time required to Fourier transform an $n \times m$ matrix from n^2m^2 to $n \log_2 m \times m \log_2 n$. This is to be compared to minutes required for the same operation when it is performed holographically. In fact, at present it seems that a maximum of 250×250 lines (i.e. image portions of about $2{\cdot}5 \times 2{\cdot}5$ mm with 100 lines/mm resolution) may be reasonably processed with current methods. However, when successful, the computer-decoded images may in the end present a perfection which may be in many ways more readily superior to that obtained by our first method. Accordingly, it may well be that the holographic deconvolution methods may serve as powerful first-step search methods, for the improvement of images, to determine the image or image sets for which further digital computer processing for image refinement may be justified. However, it appears very likely that our second 'correlative holographic decoding method' may well remain as the superior method, when it is applicable! It may also be of some interest to note analogies between these methods and some of the forms of apodization [20], and other forms of non-holographic coding and decoding, e.g. as used in spectroscopy [21–23] as well as image-sharpening methods of purely electronic nature, e.g. as used in television [24, 25], to which we have made extensive reference in the past. We also recall that optical filtering methods using filters generated by

vacuum-evaporation of dielectric films or filters generated in part in this manner and in part photographically have been described by a number of authors, notably first by Tsujiuchi [26].

2. Holographic Fourier-transform division method

Our method [1] consists in recognizing that the equation:

$$g(x,y)=f(x,y)\otimes h(x,y), \tag{25}$$

i.e. its equivalent Fourier-transform equation:

$$\bar{G}(u,v)=\bar{F}(u,v)\,\bar{H}(u,v), \tag{2}$$

may be readily solved by the Fourier-transform division:

$$\bar{G}\bar{H}^{-1}=\bar{F}, \tag{26}$$

provided that the required Fourier-transform division filter can indeed be realized. We showed in [1, 3] that such a filter could indeed be realized, notably in the form of a two-part 'sandwich'

$$\bar{H}^{-1}=\frac{\bar{H}^*}{|\bar{H}|^2}. \tag{31}$$

Each of the two filter components, $\bar{H}^*$ and $|\bar{H}|^{-2}$ can be separately realized, both from the Fourier-transform $\bar{H}(u,v)$ of the spread function $h(x,y)$, i.e. of the image of a point, as formed by the system under the conditions of use. It may be of some interest to note, for instance in connection with the diffraction patterns formed by imperfect gratings (see, e.g. [7]), that the spread function $h(x,y)$ may in fact also be readily obtained by computation (e.g. using a digital computer), when a direct measurement with adequate precision may not be readily achieved. The computation of $h(x,y)$ is based on the fact that

$$h(x,y)=\bar{E}_{\mathrm{H}}(x,y)\,\bar{E}_{\mathrm{H}}(x,y)^*, \tag{32}$$

where $\bar{E}_{\mathrm{H}}(x,y)$ is the spatial Fourier transform of the electric field 'amplitude' $\bar{E}_{\mathrm{H}}(u,v)$ in the wavefront, when the system is illuminated by a wave from a point in the object domain. The wavefront $\bar{E}_{\mathrm{H}}(u,v)$ may be readily measured interferometrically, or indeed holographically. In general, however, for most image-forming applications, the function $h(x,y)$ may in fact be determined with adequate precision simply from its photograph.

To realize, in the focal plane of a Fourier-transforming lens the field $\bar{H}(u,v)$, we must produce in the pupil of the lens the field $h(x,y)$. This may be readily achieved according to the steps involved in the negative–positive procedure leading to equation (13). Using the field $\bar{H}(u,v)$, we obtain the $\bar{H}^*$ component of the filter simply by recording the corresponding hologram, i.e. by making the $\bar{H}(u,v)$ interfere with a suitable reference field, e.g. a plane wave. We obtain a hologram in the form:

$$I(u,v)=1+|\bar{H}|^2+\bar{H}+\bar{H}^*. \tag{33}$$

Under the conditions discussed in the first section, notably in equations (15) to (24), illumination of this hologram with a wave of unit amplitude will indeed produce an imaging wave $\bar{H}^*$ as desired.

The $|\bar{H}|^{-2}$ may be obtained as follows. We first record the exposure $|\bar{H}|^2$ produced by the field $\bar{H}(u, v)$. If we now process the photographic negative with a γ equal to 2, the field transmitted through the negative will indeed be equal to $|\bar{H}|^{-2}$. We have for this field (with $\gamma = 2$):

$$\bar{E}_{\mathrm{T}} = [|\bar{H}|^2]^{-\gamma/2} = (|\bar{H}|^2)^{-1}. \tag{34}$$

Accordingly, if this field, produced by this component of the 'sandwich' filter is used to illuminate the hologram component, described by equation (33), the field transmitted in the imaging-wave side band will be:

$$|\bar{H}|^{-2}\bar{H}^* = \frac{\bar{H}^*}{|\bar{H}|^2}, \tag{35}$$

upon illumination with a unit-amplitude wave. It follows immediately that illumination of the sandwich filter with the field $\bar{G}(u, v)$ will produce an imaging wave equal to:

$$\bar{G}\frac{\bar{H}^*}{|\bar{H}|^2} = \bar{F}_{\mathrm{BL}} \cong \bar{F} \tag{36}$$

as desired. We now distinguish between the field $\bar{F}_{\mathrm{BL}}$ actually obtained by this filtering within the spatial bandwidth in which the spatial frequencies are being filtered, on the one hand, and on the other, the field $\bar{F}$ which would, correspond to a field which, by Fourier transformation would give a 'super-resolved' image $f(x, y)$, i.e. an image without any limitations such as that which would characterize even a perfectly corrected lens system, notably the 'diffraction' limitations. It may be shown [27, 28], at least mathematically, that the filtering step of equation (36) may in fact be considered as a possible first step in obtaining a certain amount of 'super-resolution' improvement, notably in cases when a suitable absence of image-degrading noise might be experimentally achievable. We hasten to note, in this context, that the situation for obtaining 'super-resolution' in such two-step (*a posteriori*) filtering appears theoretically more favourable than the situation which exists in the methods used for obtaining 'super-resolution' in one-step imaging, e.g. in radar and radio-astronomy [29, 30]. The possibility of thus investigating 'super-resolution' by two-step imaging, using holographic processing, as an example, may be of particular interest also in further progress in the application of holographic image-computing methods to the solution of the 'phase problem' in x-ray crystallography [8, 31, 32]. These preliminary considerations may be further clarified as follows. It can be shown that the Fourier-transform division indicated in equation (36) permits one to restore essentially all the spatial frequencies within the bandwidth corresponding to the image-forming aperture used to record $g(x, y)$, respectively $h(x, y)$. This is true, except for the isolated nulls of the $\bar{H}(u, v)$ function, for which the frequencies are not properly restored.

Indeed by noting that

$$h(x, y) = \bar{E}_{\mathrm{H}}(x, y)\,\bar{E}_{\mathrm{H}}(x, y)^* \tag{32}$$

and that

$$\bar{E}_{\mathrm{H}}(x, y) = \int\int_{-\infty}^{+\infty} \bar{E}_{\mathrm{H}}(u, v) \exp\,[2\pi i(ux + vy)\,du\,dv, \tag{37}$$

as we mentioned before, we immediately have (see, e.g. equation (30)):

$$\bar{H}(u, v) = \bar{E}_{\mathrm{H}}(u, v) \divideontimes \bar{E}_{\mathrm{H}}(u, v)^*, \tag{38}$$

which we may also write (see, e.g. [8, chap. III, equation (23 *b*)]) in the form:

$$\bar{H}(u,v)=\bar{E}_{\mathrm{H}}(u,v)\otimes\bar{E}_{\mathrm{H}}^{*}(-u,-v). \tag{39}$$

The filter function $\bar{H}(u,v)$ is thus in effect nothing but the 'convolution of the wavefront $\bar{E}_{\mathrm{H}}(u,v)$ with itself, according to equation (39). Since the wavefronts $\bar{E}_{\mathrm{P}}(u,v)$, perfect, and $\bar{E}_{\mathrm{H}}(u,v)$, imperfect ('blurred') occupy the same aperture both for the system 'in focus', as well as when the system is 'out of focus' (or when it 'blurrs' the image by motion) we may conclude, at least to this approximation, that the blurred spread function $h(x,y)$, as well as that $h_{\mathrm{P}}(x,y)$ which would correspond to the system 'in focus' contain *spatial frequencies up to the same limit*, in the (u,v) domain. The difference between the function $\bar{H}_{\mathrm{P}}(u,v)$, corresponding to the 'in focus' system, and the function $\bar{H}(u,v)$, corresponding to the 'blurred' spread function $h(x,y)$, is that the spatial frequencies in $\bar{H}(u,v)$ are generally smaller in amplitude, *and* shifted in phase, relative to the spatial frequencies in $\bar{H}_{\mathrm{P}}(u,v)$. It is in fact the restoration of the spatial frequencies of $\bar{H}(u,v)$ to the values in $\bar{H}_{\mathrm{P}}(u,v)$ which may be considered as the interpretation of the 'spatial filtering' restoration process. In other words, an 'in focus' system, having a 'diffraction-limited' spread function $h_{\mathrm{P}}(x,y)$ produces an image:

$$g_{\mathrm{P}}(x,y)=f(x,y)\otimes h_{\mathrm{P}}(x,y) \tag{40}$$

and also *not* a 'super-resolved' image $f(x,y)$! The field corresponding to the 'in-focus' image in the Fourier-transform domain is:

$$\bar{G}_{\mathrm{P}}(u,v)=\bar{F}(u,v)\,\bar{H}_{\mathrm{P}}(u,v), \tag{41}$$

which gives, by a second Fourier transformation (except for possible additional diffraction limitations), the field $g_{\mathrm{P}}(x,y)$, identical to that described by equation (40), and again *not* a 'super-resolved' image $f(x,y)$! Naturally, all of our previous papers implicitly made this assumption, as we explicitly stated in [1]. By comparing equations (41) and (2), it should indeed be clear that the image-deconvolution methods aim, in this first approximation, in 'restoring' the function $\bar{H}_{\mathrm{P}}(u,v)$ from the function $\bar{H}(u,v)$. Because the filtering restoration methods operate, in effect, on each spatial frequency separately, both in amplitude and in phase, it should be clear that the existence of a number of isolated zeros in the $\bar{H}(u,v)$ function, as used here for division, will not, in general, significantly affect the success of the filtering†. The existence of a number of isolated zeros in the function $\bar{H}(u,v)$, used for Fourier-transform division filtering, does not invalidate the validity of equation (26), within the limitations discussed here above. In other words, even though some of the spatial frequencies may not be restored by means of the Fourier-transform division methods, a noticeable improvement in the 'deblurred' image will in general be observed, provided that a significant part of the spatial frequency function $\bar{H}_{\mathrm{P}}(u,v)$ is indeed properly restored, in amplitude *and* in phase, especially, in many practical cases, in the lower frequency regions, inasmuch as the higher frequency regions are in general already quite attenuated in amplitude, even in perfectly corrected image-forming systems. For instance, in a perfectly corrected image forming system, using a rectangular aperture, the spatial frequency amplitudes decrease *linearly* from the lowest to the highest frequency transmitted, along a direction parallel to a side of the aperture. The

† This is essentially true in cases where there are a limited number of zero's in $\bar{H}(u,v)$, and to the extent that corresponding 'Gibbs'-like effects may be neglected in the first approximation.

'super-resolutions' which we mention above, could conceivably be obtained in a number of ways from the function $\bar{H}_{\mathrm{P}}(u, v)$. One form of 'super-resolution' which may be readily achieved, and which appears to involve few conceptual difficulties or objections, would simply consist in raising the spatial frequency amplitudes above the line of linear decrease, discussed above. Clearly, we may add, the preceding discussion refers to the formation of images, and to the recording of $g(x, y)$ in *incoherent light*, while the spatial filtering operations are, on the contrary, carried out in *coherent* light. It may be shown (see, e.g., [8]) that the spatial frequency response function, analogous to the $\bar{H}_{\mathrm{P}}(u, v)$ functions discussed above, for perfectly-corrected systems operating in *coherent light* are perfectly flat in amplitude up to a frequency equal to one-half of the cut-off frequency of incoherent-light imaging systems: at that frequency, the spatial frequency response of the coherent-light imaging systems abruptly drops to zero. It should be clear, also, that the functions $\bar{H}(u, v)$, $\bar{H}_{\mathrm{P}}(u, v)$ are nothing but the 'spatial frequency response functions' of the optical systems, in analogy with the terminology used for temporal frequency response functions in electrical circuit theory and in electronics, among others (for a general background, see, e.g., [8, Chap. III]).

Experimental verifications of the holographic Fourier-transform division method of [1] were first described by Lohmann and Werlich [2] for the deconvolution of a badly blurred image of a single 'black-on-white' point, as well as for an equally badly blurred 'black-on-white' letter 'T'. We have ourselves [3, 4] given the first experimental verifications for a 'continuous-tone' three-dimensional macroscopic object, using the theory given above. Further refinements of these methods will be given in a future publication, following completion of experiments now under way [44]. The complexity of the problem of 'realizing' (i.e. of synthesizing) such optical filters as the $\bar{H}^{-1}$ filter, equal to $\bar{H}^*/|\bar{H}|^2$, as discussed above, may perhaps be illustrated by, to some extent, comparing it to the mathematical difficulty of synthesizing electrical filters, even passive, in electronics, even when the frequency-transfer function is known. For instance, systematic methods for synthesizing RLC filters (R = resistant, L = inductance, C = capacitance), are still not known in a general way! Similarly, many years sometimes elapse before a method, such as that which we describe, is discovered in electronics for systematically synthesizing certain filter types, e.g. RL, RC or LC, especially if constraints such as 'equal values' for all resistances and all capacitances in a ladder-network may be desirable, as one example. In addition to the comparable theoretical difficulties in optics, there exists the additional difficulty resulting from the need of actually 'manufacturing' (photographically and holographically) the individual filter components, with exacting precisions, and for maintaining critical alignments of the optical-system components in the processing, as we discuss in the next section.

3. Correlative holographic decoding (deconvolution) method

It may be of interest to stress again the generality and power of the basic equations of holography first introduced by Gabor [13–15]. All the various forms of imaging and image processing, using holograms, may be shown to make use of the same fundamental 'Gabor' equations (see, e.g. [8]). However, there exists a basic difference between the *image decorrelation* (image deconvolution) methods, which we describe here, and which result in a *decoded*

(*deblurred*) *image*, on the one hand, and on the other, the image correlation methods, first introduced by Vander Lugt [41], and which result in a *coded* pattern, for instance a bright dot or a cross, indicating the location of the centre of gravity of the correlation of the area [41] or of the contour [42][43], of the 'known' pattern with the areas or contours of the patterns in the image. The Vander Lugt 'matched' filtering methods consists in *correlating* a function $f_1(x,y)$ with the best possible 'in focus' image function $f(x,y)$. The correlation may be carried out in the spatial-frequency Fourier-transform domain with the aid of a Fourier-transform hologram $[1+|\bar{F}_1|^2+\bar{F}_1+\bar{F}_1^*]$ of the coding function f_1. When the image function $f(x,y)$ is illuminated by a plane wave of coherent light, the spatial Fourier transform of $f(x,y)$ obtained in the focal plane of a lens is $\bar{F}(u,v)$ and the field transmitted through the hologram is $\bar{F}[1+|\bar{F}_1|^2+\bar{F}_1+\bar{F}_1^*]$. One of the holographic 'side-band' waves is $\bar{F}\bar{F}_1^*$ and its Fourier transform is thus equal to the *correlation* $f \overset{\times}{\times} f_1^*$, rather than to the decorrelation, as it is being sought in the image-deblurring methods! In this sense, it may be said that the image-deblurring methods aim at achieving the *solution* of an integral equation (e.g. the *solution* of equation (1) above), while the 'matched' filtering pattern-recognition methods aim at *realizing the* (in practice) much more straightforward *correlation integral*

$$\int\int_{-\infty}^{+\infty} f(x,y) f_1(x+x', y+y')\, dx\, dy = \tilde{f} \overset{\times}{\times} \tilde{f}_1.$$

For further details, see also, e.g. [8], notably also for diagrams and photographs of experimental arrangements required to materialize equations given in this paper and in references cited.

The basic principles of our new methods [5, 6] were given above in equations (27) to (30). The realization of equation (27) may be accomplished by means of two holographic schemes.

Let $g(x, y)$ be the 'blurred' photograph, such that

$$g(x,y) = f(x,y) \otimes h(x,y), \tag{25}$$

with the special requirement that the autocorrelation function of the spread function $h(x,y)$ be sharply 'peaked', i.e. that we have

$$h \overset{\times}{\times} h^* = \delta. \tag{29}$$

To this corresponds the equivalent condition:

$$\bar{H}\bar{H}^* = 1 \tag{27 a}$$

and we recall that

$$h \overset{\times}{\times} h^* \rightleftharpoons \bar{H}\bar{H}^*. \tag{30}$$

3.1. *Extended-source holographic scheme A*

Let us record the Fourier-transform hologram [8] of the function $g(x,y)$, using the photographic precautions discussed in the Introduction. The hologram is:

$$I(u,v) = 1 + |\bar{G}|^2 + \bar{G} + \bar{G}^*. \tag{42}$$

By recalling the equation:

$$\bar{G}(u,v) = \bar{F}(u,v)\bar{H}(u,v), \tag{2}$$

we may write equation (42) in the form:

$$I(u,v)=1+\bar{G}^2+\bar{F}\bar{H}+\bar{F}^*\bar{H}^*. \tag{43}$$

If we now replace the hologram into its recording position and illuminate it by the wave $\bar{H}$, originating from a suitably realized copy (see Introduction) of a photograph of the spread function $h(x,y)$, placed into the position of the point source, used to record the Fourier-transform hologram of equation (42) then the wave transmitted in the last imaging term of equation (43) (see figure 1) will be equal to

$$\bar{F}^*\bar{H}^*\bar{H}=\bar{F}^* \quad (\text{if} \quad \bar{H}\bar{H}^*=1). \tag{44}$$

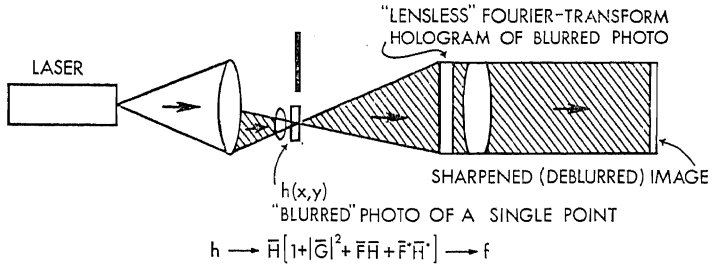

Figure 1. Arrangement used for the deconvolution of the Fourier-transform hologram of the 'blurred' photograph $g(x,y)$, for the case when the hologram was recorded with a point-source reference.

Since $\bar{F}^*$ is nothing but the complex conjugate of the imaging wave $\bar{F}$, the corresponding image, obtained by Fourier transformation in the focal plane of a lens 'looking' through the hologram is indeed equal to the desired image $f(x,y)$, upon processing of the photograph with a γ equal to -2, i.e. by printing the positive according to the condition of equation (11)†.

3.2. *Extended-source holographic scheme B*

In this case, we record the Fourier-transform hologram of $g(x,y)$ by using $h(x,y)$ as the 'extended reference source' (e.g. as in figure 27, Chap. VI of [8]). The hologram is:

$$\begin{aligned} I(u,v)&=(\bar{G}+\bar{H})(\bar{G}+\bar{H})^* \\ &=|\bar{G}|^2+|\bar{H}|^2+\bar{G}\bar{H}^*+\bar{G}^*\bar{H}. \end{aligned} \tag{45}$$

By again recalling that $\bar{G}=\bar{F}\bar{H}$, according to equation (2), we may write equation (45) in the form:

$$I(u,v)=|\bar{G}|^2+|\bar{H}|^2+\bar{F}\bar{H}\bar{H}^*+\bar{F}^*\bar{H}^*\bar{H}. \tag{46}$$

Because we are considering, in particular, the case when $\bar{H}\bar{H}^*=1$, we note that the image-forming wave of interest, say

$$\bar{F}\bar{H}\bar{H}^*=\bar{F} \quad (\text{if} \quad \bar{H}\bar{H}^*=1), \tag{47}$$

is indeed equal to $\bar{F}$ as desired. Accordingly, in this case it is sufficient to replace the hologram into its recording position, and illuminate it with a wave of unit

† In practice, this condition need not be necessarily more rigorously satisfied in this last step than in direct photography of the image $g(x,y)$, using a well-corrected system!

if the recording and reconstructing sources are the same, and if their correlation is equal to the Dirac delta, function, then equation (49) becomes:

$$T[\bar{E}_0]\otimes\delta = T[\bar{E}_0], \tag{50}$$

in agreement with the analysis of the preceding sections.

Let us now consider the simplest case of misalignment, namely the case described by equation (48). This would also be the case of interest in which $\bar{E}_R$ and $\bar{E}_{R'}$ are in fact produced by the same source, but when the source, in the reconstruction, is misaligned, so that the phase $\phi_{R'}$ is different from the phase ϕ_R, in the plane of the hologram.

In this case the imaging term of interest becomes:

$$\bar{E}_0 \exp(-i\phi_R)\exp(i\phi_{R'}) = \bar{E}_0 \exp[i(\phi_{R'}-\phi_R)], \tag{51}$$

from which we immediately recognize that the imaging wave is now not any more the wave $\bar{E}_0\lambda$, but rather a wave having a possibly very considerable wavefront aberration $(\phi_{R'}-\phi_R)$. We may recall (see, e.g. [7]) that wavefront aberrations as small as one-tenth of a wavelength (i.e. $2\pi/10$ radians $\cong 6/10$ radians) become noticeable for high-resolution imaging, when the aberration extends smoothly over large regions of the wavefront. The tolerances for more localized aberrations is about ten times smaller still, and their effect is proportional to the area of the wavefront 'covered' by the aberrations! Aberrations of several radians certainly lead to intolerably large image degradation, in the case of the 'extended' aberrations.

It is possible to assess the magnitude of the misalignment phase errors for the two types of holographic experiments discussed in the previous section.

Let us consider, for simplicity, the case of the 'lensless Fourier-transform hologram' [8, pp. 127–137], Let *one* of the waves from the reference source, located in the x plane, produce a field:

$$[\bar{E}_R(u)]_1 = \exp\left(i\frac{2\pi}{\lambda}\frac{u^2}{2f}\right) \tag{52}$$

in the hologram u plane, located at a distance f from the x plane, and parallel to it. We are assuming that the x extent of the source is small compared to the u extent of the hologram. Now let the corresponding wave from the source in the reconstruction originate from a position of the source displaced by a small distance x_0 from the position used in the recording. The reconstructing wave may then be written in the form:

$$[\bar{E}_{R'}(u)]_1 = \exp\left(i\frac{2\pi}{\lambda}\frac{(u-x_0)^2}{2f}\right). \tag{53}$$

Since we are interested in the product $\bar{E}_R{}^*\bar{E}_{R'}$, and because x_0 is small compared to u, we may write:

$$\bar{E}_R{}^*\bar{E}_{R'} \cong \exp\left(-i\frac{2\pi}{\lambda}\frac{u^2}{2f}\right)\exp\left(i\frac{2\pi}{\lambda}\frac{u^2}{2f}\right)\exp\left(-i\frac{2\pi}{\lambda}\frac{2ux_0}{2f}\right). \tag{54}$$

We may conclude that the corresponding wavefront aberration is:

$$(\phi_{R'}-\phi_R)_1 \cong \frac{2\pi}{\lambda}\frac{ux_0}{f}. \tag{55}$$

In particular, equation (55) gives the aberration at the outer 'edge' of the hologram (or of the part of the hologram used in the reconstruction).

As an example, we may consider the magnitudes involved in the experiment illustrated in figure 3.

The wavelength λ used, 6328 Å is about 1/40 000 in. The distance f used was about 33 in. The images were reconstructed using an aperture having a diameter

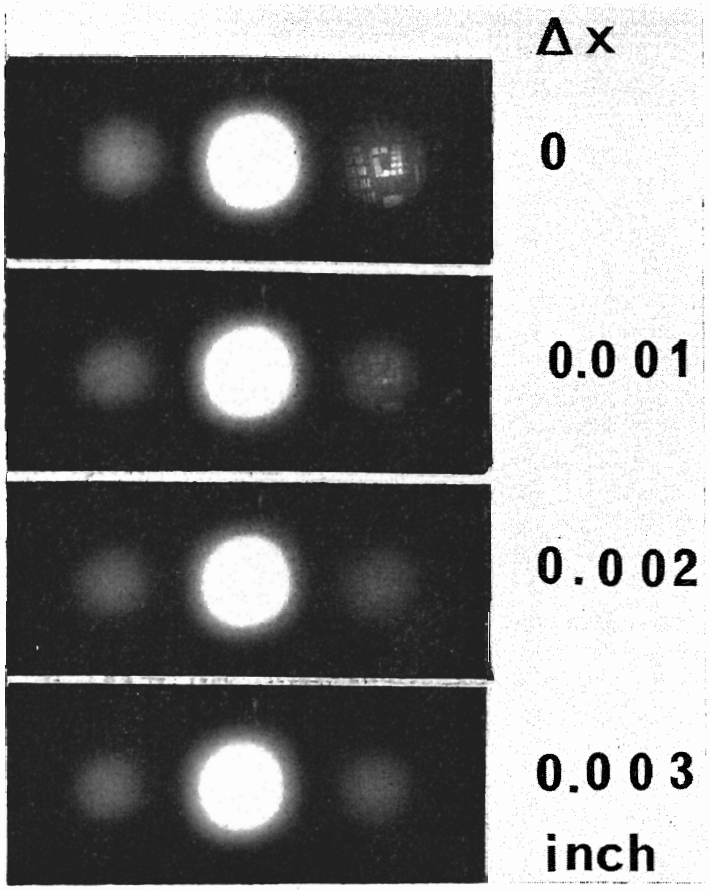

Figure 3. Experimental results showing the high degree of alignment accuracy required in the holographic image-deconvolution work (see text). The four figures, top to bottom, show the images of a test-bar target reconstructed from a hologram of the target. The hologram was recorded with an 'extended reference source' $h(x, y)$ consisting of a simple ground glass (according to a private suggestion of Gabor [40], who noted that a simple ground glass should also have the desired peaked auto-correlation function according to equation (29) in the text). The values of Δx shown refer to different positions of the hologram relative to its recording position, orthogonally to the optical z axis, at a distance of approximately 33 in. from the 'extended source' $h(x, y)$ used to illuminate it in the reconstruction, according to figure 1. The tolerances shown may also be taken to indicate the degree of similarity in the disposition of the 'centres of gravity' in the corresponding points of the spread function $h(x, y)$ and that $g(x, y)$ formed by convolution in the imaging (see text).

about 1 in. (giving $u=\frac{1}{2}$ at the edge). With a displacement $x_0=0{\cdot}001$ in., the aberration is:

$$\frac{2\pi}{\lambda}\frac{ux_0}{f}=2\pi\times 40\times 10^3\times\frac{1}{2}\times\frac{1}{10^3}\times\frac{1}{33}, \tag{56}$$

i.e.

$$\phi_{R'}-\phi_R\cong 4 \text{ radians}$$

or about two-thirds of a wavelength. By recalling the Rayleigh tolerance of about one-quarter of a wavelength for 'perfect' imaging, we should expect a displacement as small as $x_0=0{\cdot}001$ in. at a distance $f=33$ in. to produce a very noticeable deterioration in the image. This has in fact been fully borne out by our experiments, illustrated in figure 3. These results also help in explaining the results obtained in [33] carried out to verify our original method of [10, 11].

5. Image deblurring experiments using correlative holographic deconvolution

In view of verifying the theory given above, we have actually carried out a deconvolution experiment, according to scheme B (equations (45) to (47), using for the object $g(x,y)$ a computer-generated convolution (of the letter 'H') and for the spread function $h(x,y)$ a computer generated random array of 9000 pinholes (0·046 mm diameter) randomly disposed in a 17×17 mm area. The image $g(x,y)$ had its 9000 'images' disposed in the same area, and an attempt was made to have the two arrays as similar as possible, according to the tolerances of the previous section. This work, carried out in view of achieving a new method of x-ray imaging, using a multiple-pinhole camera, according to a suggestion by Dicke [34] is fully described in our ref. [16]. We did in fact obtain a perfectly convincing deconvolution of the hologram, using the method illustrated in figure 1. However, because the computer has so far not generated the functions $g(x,y)$ and $h(x,y)$ with the required alignment precision, according to our analysis, as given above†, and because actual deconvolution experiments of this type may in fact be carried out, with the small pinholes used, best at the x-ray wavelengths, for which they are designed, it appeared of interest to verify the principle of schemes A and B by holographic simulation, as follows.

We recorded in place of the hologram of the convolution

$$g(x,y)=f(x,y)\otimes h(x,y),$$

according to equation (42) the 'equivalent' hologram:

$$I(u,v)=|\bar{F}|^2+|\bar{H}|^2+\bar{F}\bar{H}^*+\bar{F}^*\bar{H}. \tag{58}$$

This is achieved by using the function $h(x,y)$ (in this case the 9000 multiple-pinhole random array mentioned above) as the 'extended' reference source in the recording of the hologram of the function $f(x,y)$ (in this case the test-bar chart, see [8, 127–137]).

By now replacing the hologram into its recording position, and by illuminating it with the wave $\bar{H}$ obtained from the 'extended' source $h(x,y)$, and by noting that this source has indeed a very sharply peaked autocorrelation function

† *Note added in proof* (21 *June* 1969): We have now successfully performed the direct verification of our theory, using a new computer-generated pair of such functions. The photographic results fully verify the theory.

(consisting of a sharp spike on a very small background, see [34], and [16], we find that the imaging wave of interest is given by the equation:

$$\bar{F}\bar{H}\bar{H}^* = \bar{F} \quad (\text{if} \quad \bar{H}\bar{H}^* = 1, \quad \text{i.e. if} \quad h \star h^* = \delta) \tag{59}$$

The imaging wave is indeed equal to $\bar{F}$, giving, by Fourier transformation, the desired 'deconvolved' image $f(x, y)$, provided that the autocorrelation function for $h(x, y)$ is satisfied, according to equation (29). The results of this experiment shown in figure 4 have fully borne out the predicted result.

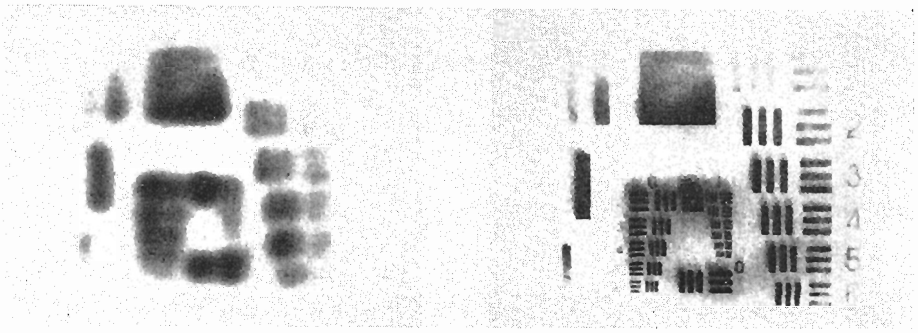

(*a*) (*b*)

Figure 4. Results of the simulation of the 'correlative holographic deconvolution method' discussed in the text. The blurred image shown in (*a*) was reconstructed by point-source illumination of the hologram formed by interference with the test-bar target function $f(x, y)$, and the 'extended-source' spread function $h(x, y)$ (see text). The deconvolved 'synthesized' image shown in (*b*) was reconstructed from the hologram by carefully replacing it into its recording position, according to figure 1, to the accuracy indicated in figure 3, and by illuminating it with the wave $\overline{H}(u, v)$ produced in its plane by the 'extended source' $h(x, y)$. The 'extended source' $h(x, y)$ used in this case was the 9000 point multiple-pinhole random array discussed in the text (see also [6, 16]).

6. Compensation of recording-medium distortions†

Because of their direct relevance to the subject discussed here, we now give some previously unpublished results of our work on three-dimensional imaging through distorting media, using our method of 'lensless Fourier-transform holography' [9]. This method (see also [8, pp. 127–137]) permits one to achieve compensation for distortions when imaging through 'turbulent' and distorting media, as was first demonstrated by Goodman *et al.* [35], and again verified by Gaskill [36], in both cases for two-dimensional objects. Because of the approximations involved in the Fourier-transform compensation (see, e.g., equation (54) above), it appeared necessary to verify to which extent tolerances, such as those corresponding to our equations (55) to (57) could be achieved in the imaging of three-dimensional objects through a 'distorting' medium. The experiments and theory are thus immediately applicable to assessing the effects of 'distortions' or deformations in the holograms, or corresponding misalignments, in terms of the applications considered here.

† Parts of this work were first presented by the author, by invitation, on 23 May 1968 at the 'Holography' Seminar of the Society of Photo-Optical Instrumentation Engineers in San Francisco, California.

Figure 5 shows a diagram of the experimental arrangement used. Let $\phi_D(u, v)$ be the distortion introduced onto a wave $\bar{E}_O(u, v)$ originating from a point of the object, as shown, where (u, v) describes the hologram plane, as before.

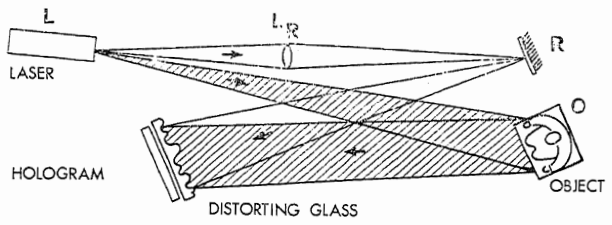

Figure 5. Lensless Fourier-transform hologram recording arrangement [9] used for compensation of wavefront deformations arising by direct imaging through 'distorting' media. L = laser (He–Ne 6328 Å), with shutter and spatial filtering pinhole. L_R = lens used to form reference point according to [9 *b*], R = reference point, O = three-dimensional object.

Let $\phi_{D'}(u, v)$ be the distortion introduced on the 'reference' wave originating from the reference point R. The imaging components in the hologram recorded according to this arrangement are thus:

$$\bar{E}_{Oi}\bar{E}_R^* \exp\left[i(\phi_{Di}-\phi_D)\right] , \tag{59}$$

for each point of the object! Comparable terms describe the imaging components for the other $(i-1)$ points of the object. It should thus be clear that 'compensation' for the distortions introduced on each object wave, and equal to $\exp[i\phi_{Di}]$, may be compensated by the distortion $\exp[i\phi_{D'}]$ introduced on the reference wave, provided that the value of the phase distortion of each wave, is compensated to the degree discussed above, i.e. say

$$\phi_{Di}-\phi_{D'} < \text{Rayleigh limit } (\pi/2 \text{ radians}) \tag{60}$$

or, more rigorously to the limits given by Maréchal [37], Toraldo di Francia [39], as well as those of the author [7], mentioned above. In particular, the Maréchal limit for good imaging would require:

$$\phi_{Di}-\phi_{D'} < \text{Maréchal limit } (\pi/4 \text{ radians}) \tag{61}$$

throughout the entire wavefront (not just locally, as mentioned above).

It should be clear also, according to this analysis, that the image obtained through the 'compensated' lensless Fourier-transform hologram will be a considerably better image than that obtained by direct photography of the object, as viewed through the distorting medium!

Our experiments, illustrated in figure 6 have fully borne out this prediction, and indeed the orders of magnitude of distortion which may be compensated according to equations (60) and (61). The uncompensated 'distorted' image, obtained by direct photography through the distorting glass is shown in figure 6 (*a*). It shows the effects of a wavefront 'distortion' estimated to be about 4 radians in a direct (laser–light) photography of the object. The image may be compared to the third image from the top in figure 3, which corresponds to a wavefront 'distortion' of about 4 radians.

The remarkable improvement obtained by the method of holographic image compensation is shown in figure 6 (*b*).

de diffraction (diffusion) qui charactérise le système optique. La deuxième méthode est encore plus directe: elle est particulièrement utilisable pour le case spécial où la fonction d'auto-correlation de la figure de diffraction (diffusion) est particulièrement pointue, ou peut être rendue particulièrement pointue. Cette dernière méthode doit permettre la réalisation d'une nouvelle classe de systèmes optiques pour les cas où l'on ne peut pas immédiatement réaliser de tels systèmes par des méthodes usuelles (par exemple en vue d'applications à l'imagerie en rayons x et en ultrasons, pour des applications d'astronomie et photographie spatiales, entre autres). Des résultats nouveaux, theoriques et expérimentaux, qui n'ont pas encore fait le sujet de publications préalables, sont présentés. Il est fait mention brève également d'applications possibles à la realisation de ' super-résolutions ' et à 'a solution du ' problème de phase ' en crystallographie avec des rayons x.

Die holographische Ortsfrequenzfilterung zur Rückgewinnung der Bilder aus zufälligen Verschmierungen und absichtlichen Verschlüsselungen zur Apertursynthese, lässt sich auf zwei Wegen erreichen. Bei dem ersten, allgemein gangbaren, benutzt man ein Trennfilter des Fourierspektrums, indem man das Hologramm der instrumentellen Streufunktion des Systems heranzieht. Der zweite, der sogar noch weiter führt, ist besonders für den speziellen Fall geeignet, in welchem die Autokorrelationsfunktion zu der Streufunktion ein scharfes Maximum besitzt oder leicht dazu gebracht werden kann. Auf diesem Wege müsste es auch möglich sein, eine neue Art optischer Systeme herzustellen, nämlich für solche Fälle, in denen die konventionellen Systeme (Linsen und Spiegel) nicht ausreichend hergestellt werden können (z.B. für Röntgen- und Ultraschallbilder, für Radioastronomie und Photographie und andere Zwecke). Die Arbeit enthält neue, bisher unveröffentlichte, theoretische und experimentelle Ergebnisse. Ferner wird auch kurz auf die Möglichkeiten eingegangen, eine " Überauflösung " zu erreichen und das Phasenproblem in der Röntgenstrahl-Kristallographie zu lösen.

References

[1] Stroke, G. W., and Zech, R. G., 1967, *Physics Lett.* A, **25,** 89.
[2] Lohmann, A. W., and Werlich, H. W., 1967, *Physics Lett.* A, **25,** 570.
[3] Stroke, G. W., Indebetouw, G., and Puech, C., 1968, *Physics Lett.* A, **26,** 443.
[4] Stroke, G. W., 1968, *Photogr. Korr.*, **104,** 82.
[5] Stroke, G. W., 1968, *Physics Lett.* A, **27,** 405.
[6] Stroke, G. W., 1968, *Physics Lett.* A, **27,** 252.
[7] Stroke, G. W., 1967, *Handbuch der Physik*, Vol. 29, edited by S. Flügge (Berlin: Springer Verlag), pp. 426–754.
[8] (*a*) Stroke, G. W., 1966, *An Introduction to Coherent Optics and Holography* (London, New York: Academic Press); (*b*) 1969, *Ibid.*, second edition (April).
[9] (*a*) Stroke, G. W., 1965, *Appl. Phys. Lett.*, **6,** 201.
(*b*) Stroke, G. W., Brumm, D., and Funkhouser, A., 1965, *J. opt. Soc. Am.*, **55,** 1327.
[10] Stroke, G. W., Restrick, R., Funkhouser, A., and Brumm, D., 1965, *Physics Lett.*, **18,** 274.
[11] Stroke, G. W., Restrick, R., Funkhouser, A., and Brumm, D., 1965, *Appl. Phys. Lett.*, **6,** 178.
[12] Maréchal, A., and Croce, P., 1953, *C. r. hebd. Séanc. Acad. Sci., Paris*, **237,** 607.
[13] Gabor, D., 1948, *Nature, Lond.*, **161,** 777.
[14] Gabor, D., 1949, *Proc. R. Soc.* A, **197,** 454.
[15] Gabor, D., 1951, *Proc. phys. Soc.*, **64,** 449.
[16] Stroke, G. W., Hoover, R. B., and Underwood, J. H., 1968, *Astrophys. J.* (submitted).
[17] Harris, J. L., 1966, *J. opt. Soc. Am.*, **56,** 569.
[18] Ansley, D., 1968, private communication to G. W. Stroke (May), based on a computation by J. W. Goodman.
[19] Cooley, J. W., and Tukey, J. W., 1965, *Math. Comput.*, **19,** 296.
[20] Jacquinot, P., and Roizen-Dossier, B., 1964, *Progress in Optics*, Vol. III, edited by Emil Wolf (Amsterdam: North-Holland Publishing Co.), pp. 31–186.
[21] Girard, A., 1963, *Optics*, **2,** 79.

[22] STROKE, G. W., and FUNKHOUSER, A., 1965, *Physics Lett.*, **16,** 272.
[23] BOUCHAREINE, P., and JACQUINOT, P., 1967, *J. Phys., Paris*, **28,** C2–183.
[24] GOLDMARK, P., and HOLLYWOOD, J. M., 1951, *Proc. Inst. Radio Engrs*, **39,** 1314.
[25] MCMANN, R., and GOLDBERG, A., 1968, *J. Soc. Motion Picture Telev. Engrs*, **77,** 221.
[26] TSUJIUCHI, J., 1963, *Progress in Optics*, Vol. II, edited by Emil Wolf (Amsterdam: North-Holland Publishing Co.), pp. 133–182.
[27] PEŘINA, J., 1968, private communication to G. W. Stroke (September).
[28] PEŘINA, J., and STROKE, G. W., 1969 *Optica Acta*, (to be submitted).
[29] TORALDO DI FRANCIA, G., 1952, *Suppl. to nuovo Cim.*, **9,** 426.
[30] SIMON, J. C., BROUSSAUD, G., and SPITZ, E., 1959, *C. r. hebd. Séanc. Acad. Sci., Paris*, **248,** 2309.
[31] STROKE, G. W., and FALCONER, D. G., 1964, *Physics Lett.*, **13,** 306.
[32] TOLLIN, P., MAIN, P., ROSSMANN, M. G., STROKE, G. W., and RESTRICK, R. C., 1966, *Nature, Lond.*, **209,** 603.
[33] LANZL, F., MAGER, H. J., and WAIDELICH, W., 1968, *Z. angew. Phys.*, **24,** 156.
[34] DICKE, R. H., 1968, *Astrophys. J.*, **153,** L–101.
[35] GOODMAN, J. W., HUNTLEY, W. H., JACKSON, D. W., and LEHMANN, M., 1966, *Appl. Phys. Lett.*, **8,** 311.
[36] GASKILL, J. D., 1968, *J. opt. Soc. Am.*, **58,** 600.
[37] MARÉCHAL, A., 1947, Thesis, Faculté des Sciences, University of Paris.
[38] TORALDO DI FRANCIA, G., 1958, *La Diffrazione della Luce*, Edizione Scientifiche Einaudi (Torino: Paolo Boringhieri).
[39] STROKE, G. W., 1967, *Modern Optics* (Proceedings of the 22–24 March 1967 Symposium) (Polytechnic Press of the Polytechnic Institute of Brooklyn), pp. 589–603.
[40] GABOR, D., 1968, private communication to the author (October).
[41] VANDER LUGT, A., 1964, *I.E.E.E. Trans. Inf. Theory*, **10,** 139.
[42] LOWENTHAL, S., and BELVAUX, Y., 1966, *C. r. hebd. Séanc. Acad. Sci., Paris*, **262,** 294; see also: 1967, *Optica Acta*, **14,** 245.
[43] VIÉNOT, J. CH., and BULABOIS, J., 1967, *Optica Acta*, **14,** 57.
[44] STROKE, G. W., 1969, *Optics Communications*, **1,** (June). This paper introduces holographic Fourier-transform division filtering using 'extended' dynamic range in the photographic filters.
[45] UPATNIEKS, J., VANDERLUGT, A., and LEITH, E. N., 1966, *Appl. Optics*, **5,** 589.
[46] TSURUTA, T., and ITOH, Y., 1968, *Appl. Optics*, **7,** 2139.